Biochemical and Biophysical Research Communications 460 (2015) 733–740

Contents lists available at ScienceDirect

Biochemical and Biophysical Research Communications

journal homepage: www.elsevier.com/locate/ybbrc

LPS-miR-34a-CCL22 axis contributes to regulatory T cell recruitment in periapical lesions

Miao He [a, b], Guangtai Song [b], Yanqin Yu [a], Qiuchen Jin [b], Zhuan Bian [a, *]

[a] The State Key Laboratory Breeding Base of Basic Science of Stomatology (Hubei-MOST) & Key Laboratory of Oral Biomedicine Ministry of Education, School & Hospital of Stomatology, Wuhan University, Wuhan 430079, China
[b] Department of Pediatric Dentistry, School and Hospital of Stomatology, Wuhan University, Wuhan 430079, China

ARTICLE INFO

Article history:
Received 8 March 2015
Available online 25 March 2015

Keywords:
microRNA-34a
CCL22
Regulatory T cell
Periapical lesions

ABSTRACT

Regulatory T cells (Tregs) have been shown to regulate the immune response and to control the defense against infection in periapical lesions, but the underlying mechanisms by which Tregs are recruited to these lesions remain unknown. Here we demonstrate that expression of the gene encoding CCL22 (also known as macrophage-derived chemokine), the major chemoattractant that recruits Tregs, is upregulated in periapical tissue during the progression of experimental periapical lesions; this upregulation positively correlated with the number of Tregs that accumulated in the lesions. In terms of mechanism, we determined that lipopolysaccharide (LPS) up-regulates *Ccl22* expression in macrophages by suppressing miR-34a. These findings suggest that the LPS-miR-34a-CCL22 axis may contribute to the recruitment of Tregs in periapical lesions, providing a potential therapeutic target for controlling this disease.

1. Introduction

Periapical lesions are caused by bacterial infection of dental pulp, leading to the infiltration of massive numbers of inflammatory cells and the development of pathogenic alveolar bone loss in jaws [1]. The balance between proinflammatory and immunoregulatory responses, which involves both the recruitment of various types of inflammatory cells and the production of cytokines/chemokines, is known to be of critical importance during the progression of periapical lesions in which $CD4^+$ T lymphocytes are the predominant infiltrating cell type [2,3]. The immune response mediated by Th17 cells plays a role in exacerbating inflammation and bone resorption in periapical lesions [4], whereas regulatory T cells (Tregs), which specifically express the transcription factor forkhead box P3 (Foxp3), infiltrate periapical lesions to suppress local inflammatory processes in order to limit tissue damage and bone destruction [1]. Previous studies have shown that Tregs infiltrate human periapical granulomas and radicular cysts, where they inhibit T-cell proliferation [5–7]. In experimental models of periapical lesions, the number of Tregs increases in a time-dependent manner [8]; an imbalance between the dynamics of $IL\text{-}17^+$ T cells and Treg dynamics may be involved in the progression of periapical lesions [9]. However, the underlying mechanisms by which Tregs are recruited to periapical lesions remain unknown.

Chemokines are a group of functionally and structurally related small proteins that may participate in the inflammation of periapical lesions by generating chemotactic gradients that are responsible for the guided migration and maintenance of Tregs [2]. C–C motif ligand 22 (CCL22), also known as macrophage-derived chemokine, was originally identified based on its secretion by macrophages and dendritic cells upon stimulation with bacterial components [10,11]. CCL22 was subsequently demonstrated to be the major chemoattractant that recruits Tregs in order to modulate the immune response in inflammation [12], autoimmune diseases [13], and tumor microenvironments [14,15].

MicroRNAs (miRNAs) are small, endogenous, non-coding RNAs that usually bind the 3'-untranslated regions (UTRs) of cognate

Abbreviations: CCL22, C–C motif ligand 22; Foxp3, forkhead box P3; LPS, lipopolysaccharide; miR-34a, microRNA-34a; qRT-PCR, quantitative reverse transcription polymerase chain reaction; TRAP, tartrate-resistant acid phosphatase; Tregs, regulatory T cells; UTRs, untranslated regions.

* Corresponding author. State Key Laboratory Breeding Base of Basic Science of Stomatology (Hubei-MOST) & Key Laboratory of Oral Biomedicine Ministry of Education, School & Hospital of Stomatology, Wuhan University, 237 Luoyu Road, Wuhan 430079, China. Fax: +86 27 87647443.
E-mail address: bianzhuan@whu.edu.cn (Z. Bian).

http://dx.doi.org/10.1016/j.bbrc.2015.03.098
0006-291X/

mRNA targets through sequence-specific interactions and are capable of suppressing gene expression post-transcriptionally by blocking translation or by degrading the target mRNA [16]. miRNAs have been associated with a wide range of physiological and pathological processes, including the inflammatory response [17]. Macrophages are critical effector cells in the host innate immune system; lipopolysaccharide (LPS) from Gram-negative bacteria in root canals reacts with monocytes/macrophages to produce various inflammatory cytokines/chemokines [18]. Several miRNAs, such as miR-101 [19], miR-125b [20], and miR-155 [21], have been shown to modulate the inflammatory reaction of macrophages, with distinct effects. miR-34a, a potent tumor suppressor, was recently identified as a regulator of the macrophage inflammatory response. LPS downregulated miR-34a expression in macrophages in a dose-dependent manner, while forced miR-34a expression suppressed the production of inflammatory cytokines in LPS-stimulated macrophages [22]. miR-34a directly targeted *Ccl22* in hepatocellular carcinoma, and persistent inhibition of miR-34a expression in liver tissue enhanced the production of CCL22, which recruits Tregs to facilitate immune escape [23].

Although innate immune cells (neutrophils and macrophages) constitute the first line of defense against infection in periapical lesions, the role of miRNAs in the pathogenesis of periapical lesions is largely unknown. Here we hypothesized that the LPS-miR-34a-CCL22 axis contributes to the accumulation of Tregs in periapical lesions.

2. Material and methods

2.1. Animals and induction of periapical lesions

Procedures for the care and use of animals were approved by the Ethics Committee of the Hospital of Stomatology, Wuhan University, Wuhan, China (protocol number: 2013-99). All applicable institutional and governmental regulations concerning the ethical use of animals were followed. Forty-eight male Sprague–Dawley rats, weighing approximately 250 g each, were purchased from the Experimental Animal Center of Wuhan University and randomly divided into four groups. All rats were anesthetized via intraperitoneal injection of pentobarbital sodium (Merck, Darmstadt, Germany; 30 mg/kg). Bilateral lower first-molar pulps were exposed to the oral environment with a #1/4 dental round bur (SS White Burs Inc., Lakewood, NJ, USA) without damaging the pulp chamber floors, as previously described [4,9]. Twelve rats in each group were sacrificed on days 0, 7, 14, and 28 after the operation. Day 0 rats served as the negative control group.

2.2. Sample preparation

Bilateral mandibles were extracted and defleshed. Half of the samples in each group were fixed in 4% paraformaldehyde at 4 °C for 48 h. Then, the specimens were demineralized in 10% ethylenediaminetetraacetic acid for 8 weeks at 4 °C. Decalcified specimens were dehydrated in an ethanol series and embedded in paraffin. Mesio-distal serial sections 6 μm in thickness were cut; those that included the patent root apex of the first mandibular molar were selected under light microscopy and subjected to histology, enzymatic histochemistry, immunohistochemistry, and immunofluorescence. The remaining samples were used for quantitative reverse transcription polymerase chain reaction (qRT-PCR). Periapical tissues surrounding the mesial and distal root apices of the first molars were carefully extracted in accordance with previous reports [24,25], rinsed in cold phosphate-buffered saline, freed of clots, and immediately placed in RNA*later*™ Storage Solution (Sigma–Aldrich, St. Louis, MO, USA).

2.3. Histology and enzymatic histochemistry

Sections stained with hematoxylin and eosin were used for the analysis of induced inflammation in periapical regions. For osteoclast identification, tartrate-resistant acid phosphatase (TRAP) activity, a relatively specific biochemical marker for osteoclasts, was detected with a TRAP kit (Sigma–Aldrich, St. Louis, MO, USA) according to the manufacturer's instruction. Sections were deparaffinized, rehydrated, incubated in a solution of naphthol AS-BI phosphoric acid and Fast Garnet GBC for 1 h at 37 °C, counterstained with hematoxylin, air dried, and mounted. Sections incubated in substrate-free medium served as negative controls. Multinuclear TRAP-positive cells were defined as osteoclasts.

2.4. Immunohistochemistry and immunofluorescence

All sections were deparaffinized through a series of xylene baths and rehydrated with graded alcohols. Antigen retrieval was performed in 10 mM sodium citrate (pH 6.0) in a water bath; samples were then placed in 3% hydrogen peroxide for 25 min to block endogenous peroxidase activity. After treatment with 3% bovine serum albumin for 30 min, sections were incubated with 1:100 rabbit anti-Foxp3 antibody (bs-0269R, Bioss Biotechnology, Beijing, China) at 4 °C overnight, incubated for 30 min with biotinylated secondary antibody, and stained with streptavidin-horseradish peroxidase complex (DAKO, Carpinteria, CA, USA) for 15 min; sections were rinsed with phosphate-buffered saline at each step. Immunostaining was visualized by developing the samples in diaminobenzidine and counterstaining with Mayer's hematoxylin. Negative controls were treated in the same fashion, but the primary antibody was omitted. Positive cells from six randomly selected areas of the periapical regions on each slide were counted by a blinded technician under 400× magnification.

For immunofluorescence, antigen retrieval was carried out as described above and the sections were incubated with 1:50 rabbit anti-Foxp3 antibody (bs-0269R, Bioss Biotechnology) or 1:50 goat anti-CCR4 antibody (sc-6127, Santa Cruz Biotechnology, Santa Cruz, CA, USA), then incubated with tetramethylrhodamine-conjugated anti-goat IgG or fluorescein isothiocyanate-conjugated anti-rabbit IgG (DAKO). Nuclei were stained with 4′,6′-diamidino-2-phenylindole. Slides were viewed with a fluorescence microscope (Leica, Germany).

2.5. qRT-PCR

Total RNA was isolated using the miRNeasy Mini Kit (Qiagen, Valencia, CA, USA) according to the manufacturer's instructions. For miRNA expression assays, total RNA was transcribed using the TaqMan miRNA Reverse Transcription Kit (Applied Biosystems, Foster City, CA, USA). To measure mRNA expression levels, 2 μg of total RNA were reverse transcribed to cDNA with the First-strand cDNA Synthesis Kit (Takara, Dalian, China). qPCR was performed using the ABI PRISM 7500 Real-Time PCR System (Applied Biosystems) with the SYBR Green/Fluorescein qPCR Master Mix (2X, Fermentas, Thermo Scientific, USA). The following primers were used: *Ccl22*, 5′-TGCTGCCAGGACTACATC-3′ and 5′-TCGGTTCTTGACGGTTAT-3′; β-actin, 5′-CACGATGGAGGGGCCGGACTCA TC-3′ and 5′-TAAAGACCTCTATGCCAACACAGT-3′; miR-34a-5p loop, 5′-TGCGCTGGCAGTGTCTTAGCTG-3′ and 5′-CTCAAGTGTCGTGGAGTCGGC AA-3′; RNU6B (U6), 5′-CGCTTCGGCAGCACATATAC-3′ and 5′-AAATATGGAA CGCTTCACGA-3′. The expression level of each gene was calculated using the $2^{-\Delta\Delta CT}$ method. Experiments were performed in triplicate.

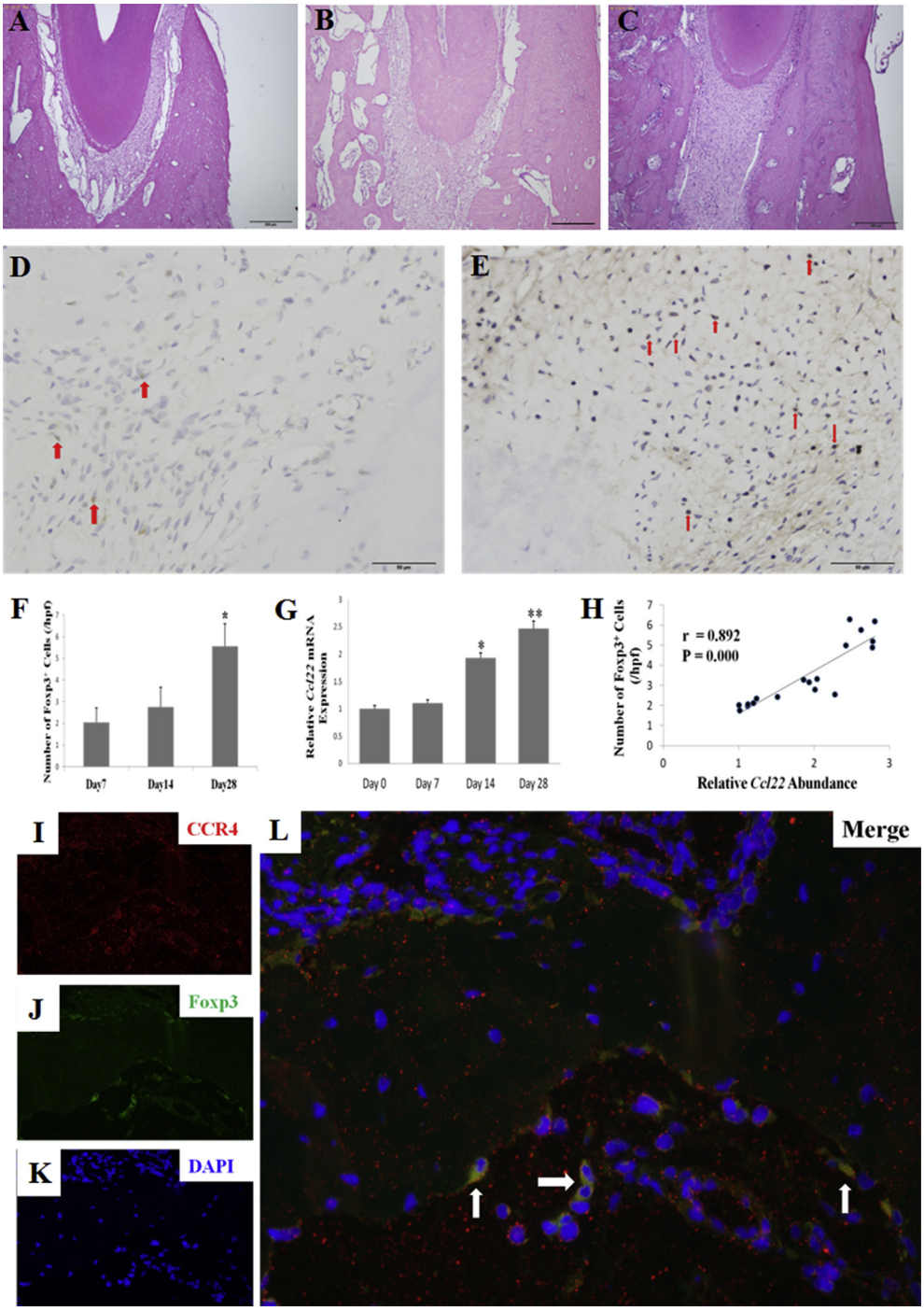

Fig. 1. Sample histology and positive correlation of elevated *Ccl22* expression with the number of Foxp3$^+$ cells in periapical lesions. (A–C) Histology of periapical regions (hematoxylin-eosin staining; original magnification, 100×; scale bars = 200 μm). (A) On day 0, periapical areas were intact and inflammation and bone destruction were not evident. (B) Infiltration of inflammatory cells and small areas of resorption of periapical alveolar bone were observed on day 14. (C) On day 28, severe inflammation and alveolar bone loss from the periapical regions occurred. (D, E) Immunohistochemistry for Foxp3 in periapical tissue on day 14 (D) and day 28 (E). Red arrows indicate Foxp3$^+$ cells. Original magnification, 400×; scale bars = 50 μm. (F) Quantitative analysis of Foxp3$^+$ cells in periapical regions (per high-power field (hpf)) on days 7, 14, and 28. The number of Foxp3$^+$ cells was significantly higher on day 28 than on other days ($^*P < 0.05$). (G) qRT-PCR of *Ccl22* mRNA expression in periapical lesions ($^*P < 0.05$; $^{**}P < 0.01$). (H) Foxp3$^+$ cell counts significantly and positively correlated with *Ccl22* expression ($r = 0.892$, $P < 0.01$). The control group contained no Foxp3$^+$ cells and was not included in the statistical analysis. (I–L) Immunofluorescent co-localization of CCR4$^+$/Foxp3$^+$ cells in a representative day-14 section. Primary antibodies against CCR4 and Foxp3 were applied to the sample, followed by incubation with tetramethylrhodamine-conjugated secondary antibody (red) against CCR4 and fluorescein isothiocyanate-conjugated secondary antibody (green) against Foxp3. Nuclei were counterstained with 4′,6′-diamidino-2-phenylindole (blue). Original magnification, 400×. (For interpretation of the references to color in this figure legend, the reader is referred to the web version of this article.)

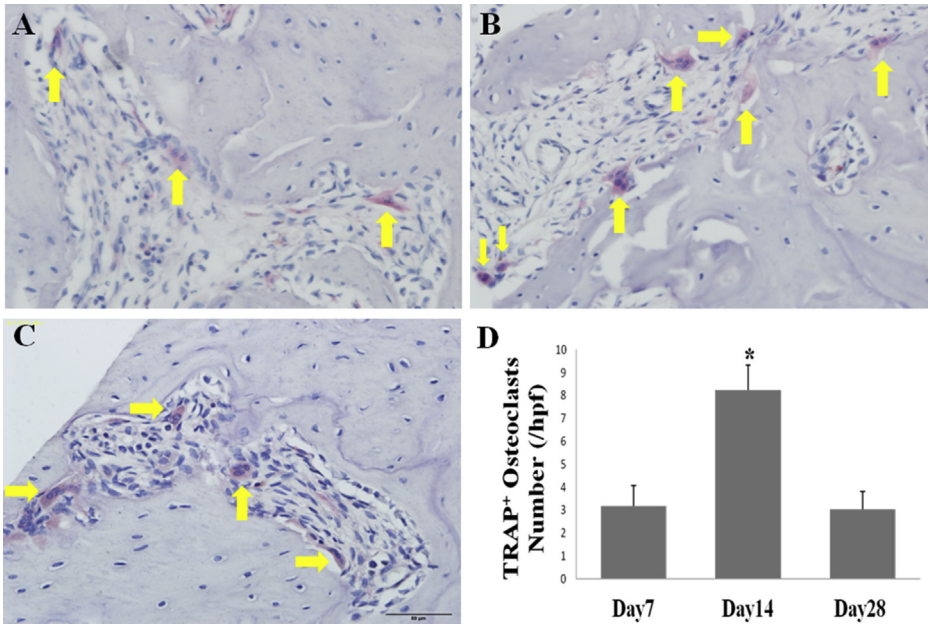

Fig. 2. TRAP staining for osteoclasts in periapical lesions. (A) Multinucleated osteoclasts started to appear in periapical lesions on day 7. (B) The number of osteoclasts increased and peaked on day 14. (C) Osteoclast numbers decreased, and few osteoclasts were visible on day 28. Arrows indicate TRAP$^+$ cells. Original magnification, 400×; scale bars = 50 μm. (D) Quantitative analysis of TRAP$^+$ cells in periapical regions (per high-power field (hpf)). The control group contained no osteoclasts and was not included in the statistical analysis. The number of TRAP$^+$ cells on day 14 was significantly higher than on days 7 and 28 (*$P < 0.05$).

2.6. Cell culture and transfection

Murine macrophage cell line RAW264.7 was purchased from the American Type Culture Collection. All cells were cultured in Dulbecco's Modified Eagle Medium with 10% fetal bovine serum, 2 μM glutamine, 100 IU/mL penicillin, and 100 μg/mL streptomycin sulfate. Cells were treated with various concentrations of ultrapure LPS from *Escherichia coli* (0, 0.1, 1, and 10 μg/mL; InvivoGen, San Diego, CA, USA) for 24 h. The murine miR-34a mimic/inhibitor and the negative control mimic/inhibitor were synthesized by GenePharma Co., Ltd (Shanghai, China). RAW264.7 cells were transfected with 50 nM of the above RNAs and Lipofectamine 2000 (Invitrogen, USA) according to the manufacturer's instructions. Transfected cells were stimulated with 1 μg/mL LPS after 24 h, and qRT-PCR was carried out 24 h later.

2.7. Luciferase assay

The 3′-UTRs of murine *Ccl22* that contain miR-34a binding sites were amplified using the specific sense primer 5′-GGCGGCTCGAGCACACACCTCCCAAGTTTC T-3′ and the antisense primer 5′-AATGCGGCCGCCCCGTTCTATTTCACAGCAA-3′ and inserted into the pmiR-RB-REPORT™ vector (Ribobio Co. Ltd., Guangzhou, China). Overlapping PCR was performed to mutate seven bases in the seed sequences of two potential miR-34a binding sites using the following primers: MUT1 sense, 5′-TGTC AGTGTGACGGTCAGTTTGTTTGGTATTAT-3′; MUT1 antisense, 5′-ACAAACT GACCGTCACACTGACACCATAGCATA-3′; MUT2 sense, 5′-ACTTTGCTGTGA CGGCATGCATGTCCTGAAGGT-3′; MUT2 antisense, 5′- CATGCATGCCGTCAC AGCAAAGTAGCACTAGTG-3′. MUT3 was generated by mutating the two miR-34a binding sites simultaneously. Assays of luciferase activity were performed 48 h after transfection using the Dual-Glo® Luciferase Assay System (Promega, Madison, WI, USA).

2.8. Statistical analysis

Analysis of variance and Pearson's correlation were performed with SPSS software for Windows release 17.0 (SPSS Inc., Chicago, IL, USA). Data are expressed as mean values ±standard deviation and $P < 0.05$ was considered statistically significant.

3. Results and discussion

3.1. Elevated expression of Ccl22 is positively correlated with the number of Foxp3$^+$ cells in periapical lesions

To determine the expression level of *Ccl22* and the number of Foxp3$^+$ Tregs in periapical lesions, we employed a well-established experimental rat model [4,9]. On day 0, periapical areas were intact and inflammation and bone destruction were not observed (Fig. 1A). Mild infiltration of inflammatory cells and small areas of resorption of the periapical alveolar bone were evident from day 7 to day 14 (Fig. 1B). On day 28, severe inflammation and alveolar bone loss from the periapical regions occurred (Fig. 1C). These histological findings were in accordance with previous reports [4,26] that periapical lesions expand rapidly between day 0 and day 14 (active phase) after pulp exposure, with slowed enlargement thereafter (chronic phase).

In periapical lesions, Tregs regulate local immune/inflammatory processes [1]. In mouse periapical lesions, Tregs are induced to infiltrate periapical tissue after pulpal exposure; previously, flow cytometry revealed that the number of Tregs increases between day 7 and day 21 in a time-dependent manner [8]. Tregs that accumulate in periapical lesions may be recruited from adjacent bone marrow or from cervical lymph nodes, where they develop from naive T cells, or may differentiate from circulating natural Tregs upon antigen stimulation [8,9]. The transcription factor Foxp3, which is expressed primarily, if not exclusively, in Tregs, is the most reliable immunohistochemical marker of Tregs [2,6,7,9].

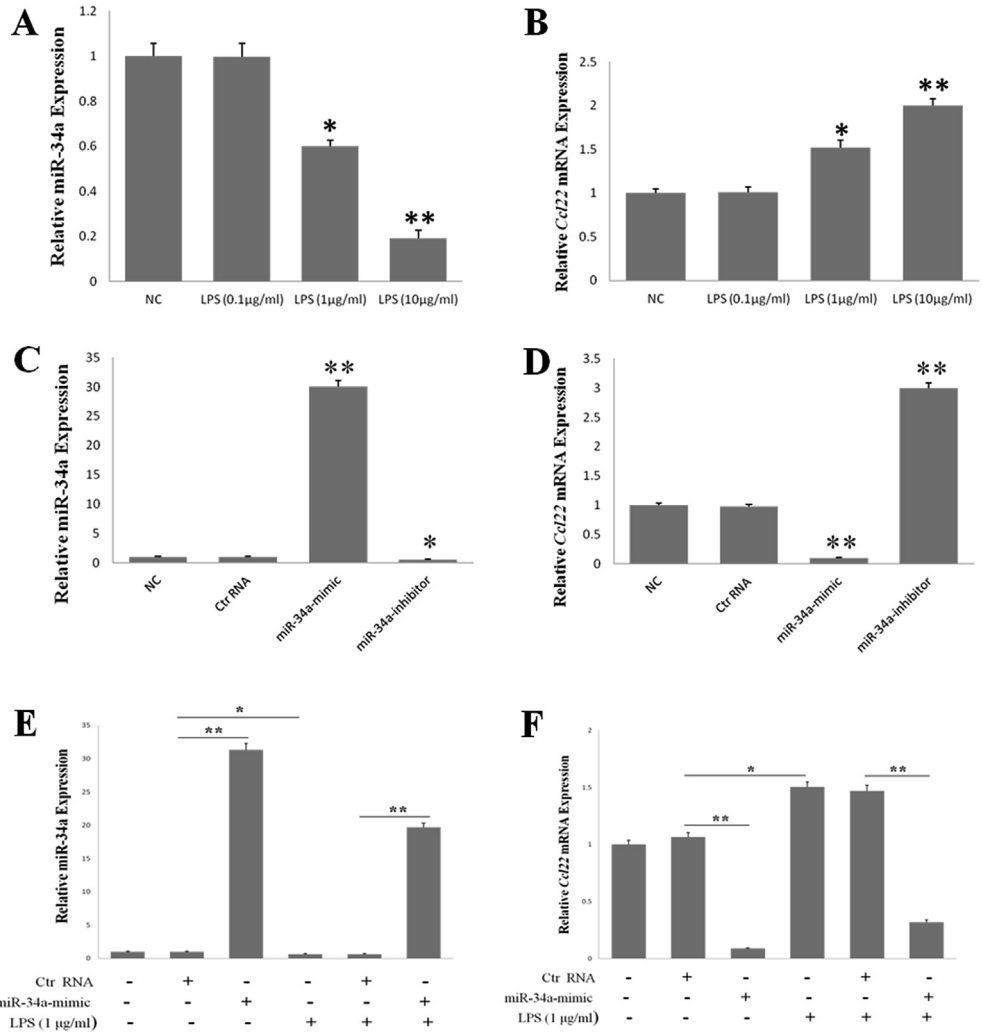

Fig. 3. LPS upregulates *Ccl22* expression in macrophages by suppressing miR-34a expression. (A, B) RAW264.7 macrophages were treated with LPS and the expression of miR-34a and *Ccl22* was analyzed via qRT-PCR. NC, negative control. (C, D) qRT-PCR of endogenous *Ccl22* expression in the presence of ectopic expression of miR-34a mimics or inhibitors. Ctr, control. (E, F) Forced miR-34a expression blocked the ability of LPS to upregulate *Ccl22* expression. $^{*}P < 0.05$ and $^{**}P < 0.01$ versus the control group.

On day 0, we did not detect Foxp3^{+} cells in periapical tissue. The number of Foxp3^{+} cells increased slowly from day 7 to day 14 (Fig. 1D), then increased rapidly until day 28 (Fig. 1E). This increase (Fig. 1F) was in agreement with previous studies [8,9], although the detection limit of our staining method and antibodies may differ from that of flow cytometry or other antibodies.

Ccl22 mRNA levels steadily increased from day 0 to day 28 after pulpal exposure, with significant differences at day 14 and day 28 compared with day 0 (Fig. 1G). Foxp3^{+} cell counts were significantly and positively correlated with *Ccl22* expression (Fig. 1H; $r = 0.892$, $P < 0.01$). Binding of the CCL22 chemokine to its receptor (CCR4) on the Treg surface recruits these immunosuppressive cells to the inflammatory microenvironment [23]. Double immunofluorescence visualized the co-localization of Foxp3^{+} and CCR4^{+} double-positive cells in the periapical region (Fig. 1I–L).

Tregs in periapical lesions secrete TGF-β, which inhibits bone resorption during osteoclast formation and differentiation [1,5]. We detected multinucleated osteoclasts in periapical lesions on day 7 (Fig. 2A). The number of osteoclasts continued to increase, peaked on day 14 (Fig. 2B), and then declined, with few osteoclasts visible on day 28 (Fig. 2C and D). The bone-protective effect of Tregs is associated with reduced osteoclast numbers and is independent of the suppression of inflammation [27]. In our study, Treg counts inversely paralleled osteoclast numbers, indicating that Tregs may help to control the expansion of periapical lesions in the chronic phase by reducing osteoclast numbers.

3.2. LPS upregulates Ccl22 expression in macrophages via suppression of miR-34a

The presence of macrophages in periapical lesions represents the host's first line of defense [3]. To assess the effect of miR-34a on *Ccl22* expression in the macrophage inflammatory reaction, we first examined changes in the expression of miR-34a and *Ccl22* in macrophages after stimulation with LPS. The murine macrophage cell line RAW264.7 was stimulated with various doses of LPS for 24 h, and miR-34a and *Ccl22* expression were analyzed via qRT-PCR. miR-34a expression was downregulated and *Ccl22* expression was upregulated after stimulation with 1 μg/mL and 10 μg/mL LPS; these changes were dose-dependent (Fig. 3A and B).

To further dissect the role of miR-34a in regulating the expression of endogenous *Ccl22*, we manipulated miR-34a expression. Ectopic expression of miR-34a mimics significantly reduced the level of *Ccl22* mRNA (Fig. 3C and D). In contrast, knocking down the

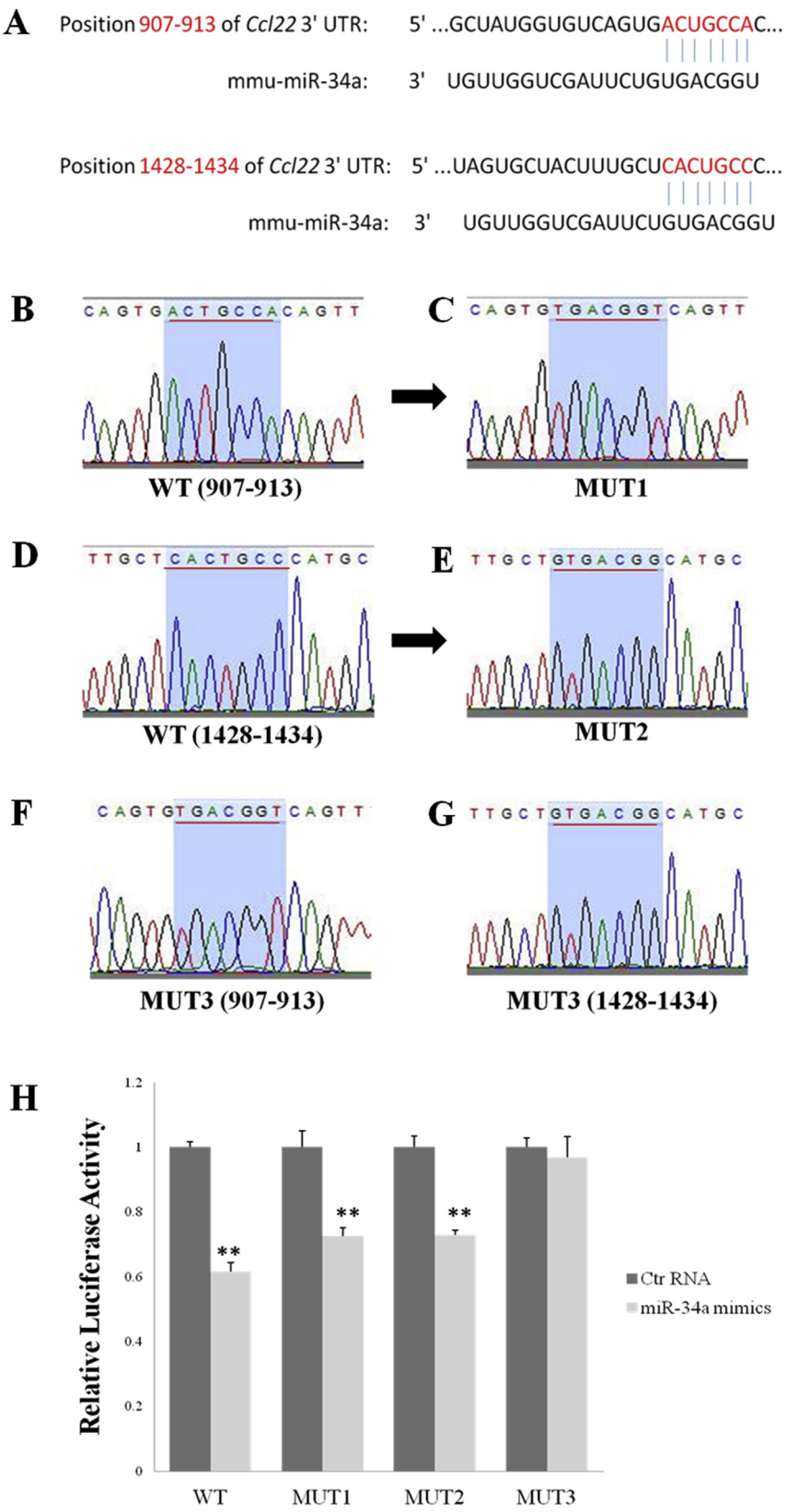

Fig. 4. Mouse *Ccl22* is a legitimate target of miR-34a. (A) Alignment of miR-34a with potential binding sites in the *Ccl22* 3′-UTR. (B–G) Seed sequences in miR-34a-binding sites of wild-type (WT) and mutant *Ccl22* 3′-UTR constructs were verified by direct sequencing. (H) Luciferase assays showed that miR-34a controls *Ccl22* expression through these putative targeting sequences. $^{**}P < 0.01$ versus the control group. Ctr, control; WT, wildtype.

endogenous expression of miR-34a with miR-34a inhibitors dramatically upregulated the level of *Ccl22* mRNA. miR-34a expression was inversely correlated with that of *Ccl22*, suggesting that miR-34a may directly target *Ccl22*. Next, we measured miR-34a levels in periapical lesions to determine whether miR-34a and *Ccl22* levels are inversely related during the development of periapical lesions. Unexpectedly, miR-34a expression at day 7 was upregulated by ~1.5 fold compared with day 0. From day 14 to day 28, miR-34a levels gradually decreased below the day-0 level (data not shown). These data suggest that during the early development of periapical lesions, miR-34a expression is regulated by other factors in addition to LPS.

We then tested whether LPS induced *Ccl22* expression in macrophages via suppression of miR-34a. Forced miR-34a expression abrogated the ability of LPS to upregulate *Ccl22* expression in macrophages (Fig. 3E and F), suggesting that the effect of LPS on *Ccl22* expression is predominantly mediated by the suppression of miR-34a expression.

3.3. Murine Ccl22 is a bona-fide target of miR-34a

The functional targets of a certain miRNA may change in various cell types or under various physiopathological conditions in order to accomplish different biological functions [22]. In this study, we applied a combination of bioinformatics and experimental approaches to further validate *Ccl22* as a legitimate target of miR-34a in the macrophage inflammatory response. Potential miR-34a-targeting seed sequences in the 3′-UTR of murine *Ccl22* (gene ID 20299) were predicted with established bioinformatic procedures [28,29] (Fig. 4A). There are two putative miR-34a binding sites in the 3′-UTR of *Ccl22*. To determine whether miR-34a controls *Ccl22* expression through these putative targeting sequences, we carried out a luciferase assay with these elements. A wild-type construct of the *Ccl22* 3′-UTR was generated, and the two putative miR-34a seed sites were mutated separately (MUT1, MUT2) or simultaneously (MUT3). All constructs were verified by Sanger sequencing (Fig. 4B–G). miR-34a mimic RNAs significantly suppressed the luciferase activity of the wild-type reporter and had less strong but still significant effects on the MUT1 and MUT2 reporters (Fig. 4H). miR-34a mimic RNAs had minimal effect on the MUT3 reporter (Fig. 4H), indicating that murine *Ccl22* is a bona-fide target of miR-34a.

In summary, our investigation clearly demonstrates that elevated *Ccl22* expression is positively correlated with the number of Foxp3$^+$ Tregs in periapical lesions. LPS downregulates miR-34a expression, causing the upregulation of *Ccl22* expression in macrophages. These findings indicate that the LPS-miR-34a-CCL22 axis may underlie Treg recruitment to periapical lesions, providing potential therapeutic targets for controlling this disease.

Conflict of interest

None.

Acknowledgments

This study was supported by the National Natural Science Foundation of China (81300870).

Transparency document

Transparency document related to this article can be found online at http://dx.doi.org/10.1016/j.bbrc.2015.03.098.

References

[1] M. Colic, D. Gazivoda, D. Vucevic, I. Majstorovic, S. Vasilijic, R. Rudolf, Z. Brkic, P. Milosavljevic, Regulatory T-cells in periapical lesions, J. Dent. Res. 88 (2009) 997–1002.
[2] J.R.B. Marcal, R.O. Samuel, D. Fernandes, M.S. de Araujo, M.H. Napimoga, S.A.L. Pereira, J.T. Clemente-Napimoga, P.M. Alves, R. Mattar, V. Rodrigues Jr., D.B.R. Rodrigues, T-helper cell type 17/regulatory T-cell immunoregulatory balance in human radicular cysts and periapical granulomas, J. Endod. 36 (2010) 995–999.
[3] M. Colic, D. Gazivoda, D. Vucevic, S. Vasilijic, R. Rudolf, A. Lukic, Proinflammatory and immunoregulatory mechanisms in periapical lesions, Mol. Immunol. 47 (2009) 101–113.
[4] H. Xiong, L. Wei, B. Peng, Immunohistochemical localization of IL-17 in induced rat periapical lesions, J. Endod. 35 (2009) 216–220.
[5] T.B. Teixeira-Salum, D.B.R. Rodrigues, A.M. Gervasio, C.J.A. Souza, V. Rodrigues Jr., A.M. Loyola, Distinct Th1, Th2 and Treg cytokines balance in chronic periapical granulomas and radicular cysts, J. Oral Pathol. Med. 39 (2010) 250–256.
[6] R.F. Peixoto, J.S. Pereira, C.F.W. Nonaka, E.J.D. Silveira, M.C.C. Miguel, Immunohistochemical analysis of FoxP3$^+$ cells in periapical granulomas and radicular cysts, Arch. Oral. Biol. 57 (2012) 1159–1164.
[7] A.L.D.L. Andrade, C.F.W. Nonaka, M.A. Gordon-Nunez, R.A. Freitas, H.C. Galvao, Immunoexpression of interleukin 17, transforming growth factor β1, and forkhead box P3 in periapical granulomas, radicular cysts, and residual radicular cysts, J. Endod. 39 (2013) 990–994.
[8] E. AlShwaimi, P. Purcell, T. Kawai, H. Sasaki, M. Oukka, A. Campos-Neto, P. Stashenko, Regulatory T cells in mouse periapical lesions, J. Endod. 35 (2009) 1229–1233.
[9] S. Yang, L. Zhu, L. Xiao, Y. Shen, L. Wang, B. Peng, M. Haapasalo, Imbalance of interleukin-17$^+$ T-cell and Foxp3$^+$ regulatory T-cell dynamics in rat periapical lesions, J. Endod. 40 (2014) 56–62.
[10] H. Ghadially, X. Ross, C. Kerst, J. Dong, A.B. Reske-Kunz, R. Ross, Differential regulation of CCL22 gene expression in murine dendritic cells and B cells, J. Immunol. 174 (2005) 5620–5629.
[11] R.J.T. Rodenburg, R.F.B. Brinkhuis, R. Peek, J.R. Westphal, F.H.J. Van Den Hoogen, W.J. van Venrooij, L.B.A. van de Putte, Expression of macrophage-derived chemokine (MDC) mRNA in macrophages is enhanced by interleukin-1β, tumor necrosis factor α, and lipopolysaccharide, J. Leukoc. Biol. 63 (1998) 606–611.
[12] J. Riezu-Boj, E. Larrea, R. Aldabe, L. Guembe, N. Casares, E. Galeano, I. Echeverria, P. Sarobe, I. Herrero, B. Sangro, J. Prieto, J. Lasarte, Hepatitis C virus induces the expression of CCL17 and CCL22 chemokines that attract regulatory T cells to the site of infection, J. Hepatol. 54 (2011) 422–431.
[13] J. Montane, L. Bischoff, G. Soukhatcheva, D.L. Dai, G. Hardenberg, M.K. Levings, P.C. Orban, T.J. Kieffer, R. Tan, C.B. Verchere, Prevention of murine autoimmune diabetes by CCL22-mediated Treg recruitment to the pancreatic islets, J. Clin. Invest. 121 (2011) 3024–3028.
[14] Y. Mizukami, K. Kono, Y. Kawaguchi, H. Akaike, K. Kamimura, H. Sugai, H. Fujii, CCL17 and CCL22 chemokines within tumor microenvironment are related to accumulation of Foxp3$^+$ regulatory T cells in gastric cancer, Int. J. Cancer 122 (2008) 2286–2293.
[15] M. Gobert, I. Treilleux, N. Bendriss-Vermare, T. Bachelot, S. Goddard-Leon, V. Arfi, C. Biota, A.C. Doffin, I. Durand, D. Olive, S. Perez, N. Pasqual, C. Faure, I. Ray-Coquard, A. Puisieux, C. Caux, J. Blay, C. Menetrier-Caux, Regulatory T cells recruited through CCL22/CCR4 are selectively activated in lymphoid infiltrates surrounding primary breast tumors and lead to an adverse clinical outcome, Cancer Res. 69 (2009) 2000–2009.
[16] H. Liu, S. Zhang, H. Lin, R. Jia, Z. Chen, Identification of microRNA–RNA interactions using tethered RNAs and streptavidin aptamers, Biochem. Biophys. Res. Commun. 422 (2012) 405–410.
[17] M.A. Lindsay, microRNAs and the immune response, Trends Immunol. 29 (2008) 343–351.
[18] M. Fujihara, M. Muroi, K. Tanamoto, T. Suzuki, H. Azuma, H. Ikeda, Molecular mechanisms of macrophage activation and deactivation by lipopolysaccharide: roles of the receptor complex, Pharmacol. Ther. 100 (2003) 171–194.
[19] Q.Y. Zhu, Q. Liu, J.X. Chen, K. Lan, B.X. Ge, MicroRNA-101 targets MAPK phosphatase-1 to regulate the activation of MAPKs in macrophages, J. Immunol. 185 (2010) 7435–7442.
[20] A.J. Murphy, P.M. Guyre, P.A. Pioli, Estradiol suppresses NF-kappa B activation through coordinated regulation of let-7a and miR-125b in primary human macrophages, J. Immunol. 184 (2010) 5029–5037.
[21] R.M. O'Connell, K.D. Taganov, M.P. Boldin, G. Cheng, D. Baltimore, MicroRNA-155 is induced during the macrophage inflammatory response, Proc. Natl. Acad. Sci. U. S. A. 104 (2007) 1604–1609.
[22] P. Jiang, R. Liu, Y. Zheng, X. Liu, L. Chang, S. Xiong, Y. Chu, MiR-34a inhibits lipopolysaccharide-induced inflammatory response through targeting Notch1 in murine macrophages, Exp. Cell Res. 318 (2012) 1175–1184.
[23] P. Yang, Q.J. Li, Y. Feng, Y. Zhang, G.J. Markowitz, S. Ning, Y. Deng, J. Zhao, S. Jiang, Y. Yuan, H.Y. Wang, S.Q. Cheng, D. Xie, X.F. Wang, TGF-β-miR-34a-CCL22 signaling-induced Treg cell recruitment promotes venous metastases of HBV-positive hepatocellular carcinoma. Cancer Cell 22 (2012) 291–303.
[24] L. Wang, R. Zhang, B. Peng, Expression of a novel PDGF isoform, PDGF-C, in experimental periapical lesions, J. Endod. 35 (2009) 377–381.

[25] Z. Sun, L. Wang, B. Peng, Kinetics of glycogen synthase kinase (GSK) 3β and phosphorylated GSK3β (Ser 9) expression in experimentally induced rat periapical lesions, Int. Endod. J. 47 (2014) 1107–1116.
[26] L. Wang, B. Peng, Correlation between platelet-derived growth factor B chain and bone resorption in rat periapical lesions, J. Endod. 33 (2007) 709–711.
[27] M.M. Zaiss, B. Frey, A. Hess, J. Zwerina, J. Luther, F. Nimmerjahn, K. Engelke, G. Kollias, T. Hünig, G. Schett, J.P. David, Regulatory T cells protect from local and systemic bone destruction in arthritis, J. Immunol. 184 (2010) 7238–7246.
[28] B.P. Lewis, I.H. Shih, M.W. Jones-Rhoades, D.P. Bartel, C.B. Burge, Prediction of mammalian microRNA targets, Cell 115 (2003) 787–798.
[29] M.R. ehmsmeier, P. Steffen, M. Hochsmann, R. Giegerich, Fast and effective prediction of microRNA/target duplexes, RNA 10 (2004) 1507–1517.